Photoinduced Energy and Electron-Transfer Processes in Porphyrin−Perylene Bisimide Symmetric Triads

Marco Ghirotti,[†] Claudio Chiorboli,[‡,§] Chang-Cheng You,[||] Frank Würthner,*[,||] and Franco Scandola*[,†,§]

Dipartimento di Chimica, Università di Ferrara, 44100 Ferrara, Italy, ISOF-CNR, Sezione di Ferrara, 44100 Ferrara, Italy, INSTM, Sezione di Ferrara, 44100 Ferrara, Italy, and Institut für Organische Chemie, Universität Würzburg, 97074 Würzburg, Germany

Received: November 16, 2007; In Final Form: January 14, 2008

The photophysics of two symmetric triads, $(ZnP)_2PBI$ and $(H_2P)_2PBI$, made of two zinc or free-base porphyrins covalently attached to a central perylene bisimide unit has been investigated in dichloromethane and in toluene. The solvent has been shown to affect not only quantitatively but also qualitatively the photophysical behavior. A variety of intercomponent processes (singlet energy transfer, triplet energy transfer, photoinduced charge separation, and recombination) have been time-resolved using a combination of emission spectroscopy and femtosecond and nanosecond time-resolved absorption techniques yielding a very detailed picture of the photophysics of these systems. The singlet excited state of the lowest energy chromophore (perylene bisimide in the case of $(ZnP)_2PBI$, porphyrin in the case of $(H_2P)_2PBI$) is always quantitatively populated, besides by direct light absorption, by ultrafast singlet energy transfer (few picosecond time constant) from the higher energy chromophore. In dichloromethane, the lowest excited singlet state is efficiently quenched by electron transfer leading to a charge-separated state where the porphyrin is oxidized and the perylene bisimide is reduced. The systems then go back to the ground state by charge recombination. The four charge separation and recombination processes observed for $(ZnP)_2PBI$ and $(H_2P)_2PBI$ in dichloromethane take place in the sub-nanosecond time scale. They obey standard free-energy correlations with charge separation lying in the normal regime and charge recombination in the Marcus inverted region. In less polar solvents, such as toluene, the energy of the charge-separated states is substantially lifted leading to sharp changes in photophysical mechanism. With $(ZnP)_2PBI$, the electron-transfer quenching is still fast, but charge recombination takes place now in the nanosecond time scale and to triplet state products rather than to the ground state. Triplet−triplet energy transfer from the porphyrin to the perylene bisimide is also involved in the subsequent deactivation of the triplet manifold to the ground state. With $(H_2P)_2PBI$, on the other hand, the driving force for charge separation is too small for electron-transfer quenching, and the deactivation of the porphyrin excited singlet takes place via intersystem crossing to the triplet followed by triplet energy transfer to the perylene bisimide and final decay to the ground state.

Introduction

Because of their structural analogy to chlorophylls, porphyrins and metalloporphyrins (**1**, with M = H_2 or metal, respectively) have been extensively used in the design of bioinspired systems for artificial photosynthesis. Thus, a large number of donor−acceptor[1] and multichromophoric systems[2] based on porphyrins have been designed to emulate the charge separation and the antenna functions of reaction centers[3] and light-harvesting complexes[4] of natural photosynthetic membranes.[5] The synthetic flexibility of this type of chromophore is convenient from this viewpoint. The excited-state and redox properties can be easily tuned over wide ranges by metalation and by appropriate selection of the R_1-R_4 substituents. Moreover, a variety of binding motifs is available for assembling these building blocks into supramolecular structures. In addition to covalent bonding through the mesopositions, coordinative bonds between peripheral ligands and metal centers can be used to connect porphyrin building blocks leading to supramolecular systems of remarkable structural variety.[6−10]

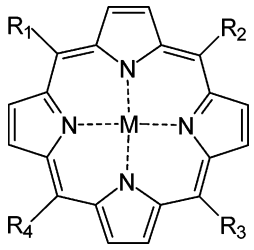

1

Another class of organic chromophores that has received considerable attention in the same area is that of aromatic bisimides and particularly perylene bisimides of general formula **2**. Though structurally very different, these dyes exhibit several functional analogies to porphyrins and chlorophylls.[11] Their excited-state and redox properties can be easily tuned by chemical design in particular by appropriate choice of the substituents R_3-R_6 in the "bay" area.[12] Thus, a large number

* To whom correspondence should be addressed. E-mail: snf@unife.it.
† Università di Ferrara.
‡ ISOF-CNR, Sezione di Ferrara.
§ INSTM, Sezione di Ferrara.
|| Universität Würzburg.

10.1021/jp7109516 CCC: $40.75
Published on Web 03/12/2008

of functional systems and assemblies based on perylene bisimides have been developed.[11−14]

Several mixed systems, containing both porphyrins and perylene bisimides, have also been studied with particular regard to the occurrence of energy and electron-transfer processes between the two types of molecular components[15−19] and to charge migration in higher-order supramolecular

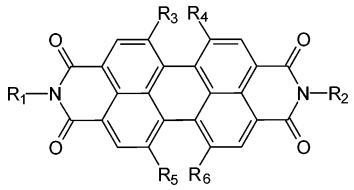

2

aggregates of such species.[15b,d,e] The various types of porphyrin−perylene bisimide conjugates differ in the state of metalation and in the mesosubstituents of the porphyrins (M = Zn or 2H, R_1-R_4 = alkyl of phenyl derivatives) and in the N,N′ or bay region substituents of the perylene bisimides (R_1, R_2 = alkyl of phenyl derivatives, R_3-R_6 = H, phenoxy derivatives). The connections between the two types of units always involve the mesopositions of the porphyrin while, on the perylene bisimide side, it can take place either at the imide nitrogens or at the carbons of the bay area.

In this article, we report a detailed photophysical characterization of the trichromophoric systems $(ZnP)_2PBI$ and $(H_2P)_2$-PBI. These symmetric three-component systems will be indicated throughout the paper as "triads", although they are obviously pseudodyads from a functional viewpoint. The synthesis and spectroscopic characterization of $(ZnP)_2PBI$ have previously been reported.[17] These systems are similar in terms of connecting motif, though different in detailed chromophore substituent pattern, to some of the systems recently developed by Wasielewski and co-workers.[15b−e]

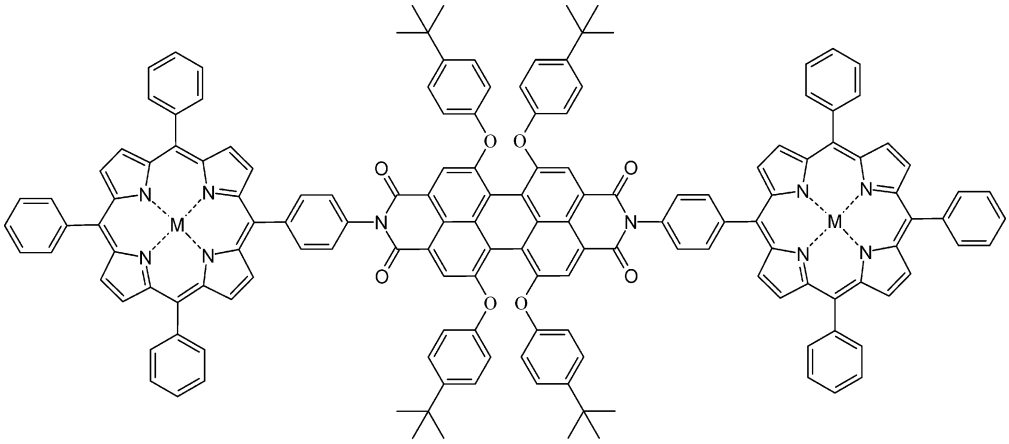

$(H_2P)_2PBI$ M = 2H
$(ZnP)_2PBI$ M = Zn

Experimental Section

Materials. The $(H_2P)_2PBI$ and $(ZnP)_2PBI$ triads were synthesized, purified, and characterized as previously described.[17] The solvents were of spectroscopy grade and were used as received.

Apparatus. UV−vis absorption spectra were recorded with a Perkin-Elmer Lambda 40 spectrophotometer. Emission spectra were taken on a Spex Fluoromax-2 spectrofluorimeter equipped with Hamamatsu R3896 tubes. The emission spectra were corrected for the instrumental response by calibration with a National Bureau of Standards standard quartz-halogen lamp.

Cyclic voltammetric measurements were carried out with a PC-interfaced Eco Chemie Autolab/Pgstat30 Potentiostat. Argon-purged 10^{-4} M sample solutions in CH_2Cl_2 (Romil, Hi-dry), containing 0.1 M [TBA]PF6 (Fluka, electrochemical grade, 99%; dried in an oven), were used. A conventional three-electrode cell assembly was used: a saturated calomel electrode (SCE, L 6 mm, AMEL) and a platinum wire, both separated from test solution by a frit, were used as reference and counter electrodes, respectively, and a glassy carbon electrode (8 mm2, AMEL) was used as a working electrode. The scan rate was 200 mV/s.

Nanosecond emission lifetimes were measured using a TCSPC apparatus (PicoQuant Picoharp300) equipped with sub-nanosecond LED sources (280−600 nm range, 500−700 ps pulsewidth) powered with a PicoQuant PDL 800-B variable (2.5−40 MHz) pulsed power supply. The decays were analyzed by means of PicoQuant FluoFit Global Fluorescence Decay Analysis software.

Nanosecond transient absorption spectra and lifetimes were measured with an Applied Photophysics laser flash photolysis apparatus, with frequency doubled (532 nm, 330 mJ) or tripled (355 nm, 160 mJ), Surelite Continuum II Nd/YAG laser (half-width 6−8 ns). Photomultiplier (Hamamatsu R928) signals were processed by means of a LeCroy 9360 (600 MHz, 5 Gs/sec) digital oscilloscope.

Femtosecond time-resolved experiments were performed using a pump−probe setup on the basis of the Spectra-Physics Hurricane Ti:sapphire laser source and the Ultrafast Systems Helios spectrometer.[20] The 560 nm pump pulses were generated with a Spectra Physics 800 OPA. Probe pulses were obtained by continuum generation on a sapphire plate (useful spectral range, 440−800 nm). Effective time resolution was ca. 300 fs, temporal chirp over the white light 440−800 nm range was ca. 200 fs, and temporal window of the optical delay stage was 0−1000 ps. The time-resolved spectral data were analyzed with the Ultrafast Systems Surface Explorer Pro software.

Procedures. All the photophysical experiments were performed in freshly prepared solutions. The stability of the solutions was spectrophotometrically checked before and after each experiment. The halocarbon solvents were previously saturated with potassium carbonate to remove traces of acidity, which were found to alter absorption spectra of the free-base

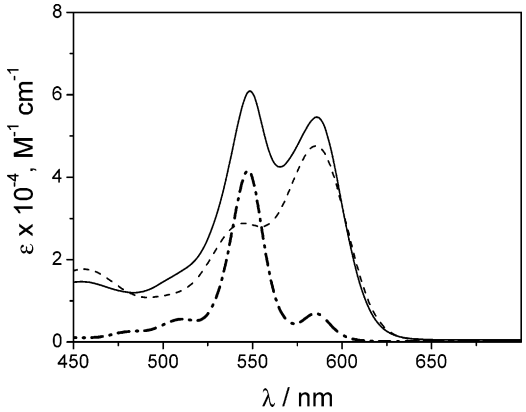

Figure 1. Absorption spectra of $(ZnP)_2PBI$ (continuous line), DPyPBI (dashed line), and ZnTPP (dash−dot line, molar absorptivity values × 2) in dichloromethane.

species and to promote photodecomposition under prolonged laser irradiation.

Results and Discussion

The photophysical behavior of the $(H_2P)_2PBI$ and $(ZnP)_2PBI$ has been fully characterized both in dichloromethane and in toluene. Some kinetic measurements have also been performed, for purposes of comparison, in chloroform. The results are discussed by comparison with those obtained in previous work for 5,10,15,20-tetraphenylporphyrin (TTP), zinc 5,10,15,20-tetraphenylporphyrin (ZnTPP), and *N*,*N*′-di(4-pyridyl)-1,6,7,-12-tetra(4-tert-butylphenoxy)perylene-3,4:9,10-tetracarboxylic acid bisimide (DPyPBI)[19] as convenient models of the H_2P, ZnP, and PBI subunits of the triads. Each triad will be first discussed separately. Then, a comparison between the results obtained with the two triads will be made.

Photophysics of $(ZnP)_2PBI$. The absorption spectrum in dichloromethane of $(ZnP)_2PBI$ is compared in Figure 1 with those of the DPyPBI and ZnTPP fragment models. It can be seen that, aside from small differences in the band intensities, the spectrum of the adduct is a good superposition of those of the molecular components. This indicates that the electronic interaction between the molecular components in the supramolecular adduct is weak and permits a reasonable estimation of the amount of light absorbed by the two types of chromophores at the various wavelengths. In practice, 585 nm is a convenient wavelength for efficient (90%) excitation of the perylene chromophore while selective excitation of the porphyrin chromophore is more difficult (at best, 60% at 550 nm). The spectral features of Figure 1 remain almost unchanged by changing the solvent from dichloromethane to toluene with the only difference being a small blue shift (from 586 to 578 nm) of the perylene bisimide absorption band.

The supramolecular nature of $(ZnP)_2PBI$ allows us to construct the energy-level diagram of Figure 2 from known properties of the molecular components. In particular, singlet energies are taken from the fluorescence of DPyPBI and ZnTPP (see below), and triplet energies are taken from literature data[21,22] on the same model systems. Besides the energy levels of the molecular components, Figure 2 includes also a charge-separated state where a zinc porphyrin is oxidized and the perylene bisimide unit is reduced. The energy of such a state (1.46 eV) is obtained[23] from the known redox potentials of the models DPyPBI (−0.69 vs SCE in CH_2Cl_2)[8,24,25] and ZnTPP (0.88 V vs SCE in CH_2Cl_2)[8] with appropriate correction for the electrostatic work term estimated according to standard procedures.[26] In terms of possible intercomponent processes, Figure 2 indicates that in $(ZnP)_2PBI$ singlet energy transfer is energetically allowed from zinc porphyrin to perylenebisimide, while electron-transfer quenching is substantially exergonic for both excited chromophores.

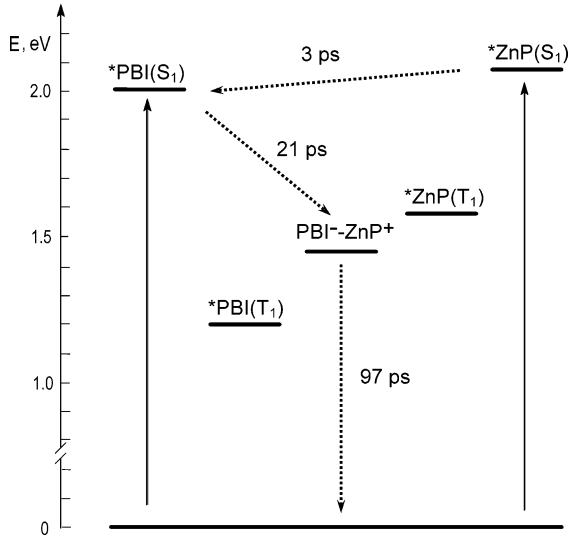

Figure 2. Energy-level diagram for $(ZnP)_2PBI$ in dichloromethane. Observed intramolecular photophysical processes (see below) are indicated by dotted arrows.

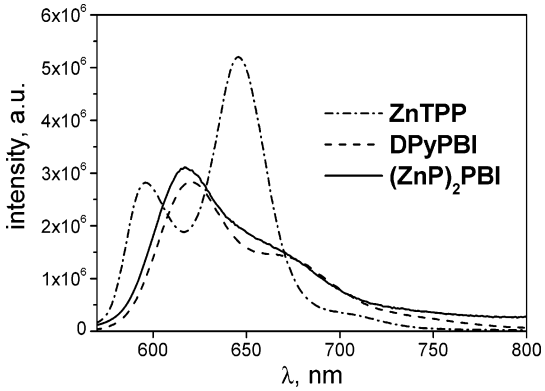

Figure 3. Emission spectra of $(ZnP)_2PBI$ (continuous line), DPyPBI (dashed line), and ZnTPP (dash−dot line) in dichloromethane.

The emission spectra of $(ZnP)_2PBI$, DPyPBI, and ZnTPP in dichloromethane are compared, on an arbitrary intensity scale, in Figure 3. It is clearly seen that the weak (see below) emission of $(ZnP)_2PBI$ is fluorescence from the perylene bisimide chromophore. The excitation spectrum of this emission (see Figure S1 of supporting material) is nicely superimposable to the absorption spectrum of $(ZnP)_2PBI$ in the whole spectral region of Figure 1. This indicates that singlet energy transfer from the porphyrin chromophores to the perylene bisimide unit, *ZnP(S_1) → *PBI(S_1) in Figure 2, is very efficient. The process, expected to take place in ca. 5 ps on the basis of Förster-type calculations,[27,28] is indeed ultrafast (time constant of 3 ps as measured by femtosecond spectroscopy with 550 nm excitation).[29] It must be stressed that the perylene bisimide fluorescence in $(ZnP)_2PBI$ is much weaker than that of free perylene bisimide with a quenching ratio of ca. 300 estimated from optically matched solutions of DPyPBI and $(ZnP)_2PBI$ (excitation wavelength, 586 nm). Since the lifetime of the DPyPBI fluorescence is 7.2 ns,[19] the perylene bisimide emission in $(ZnP)_2PBI$ is expected to be very short-lived (ca 20−30 ps). As a matter of fact, no transient emission can be observed for $(ZnP)_2PBI$ with a single-photon lifetime apparatus that has 300

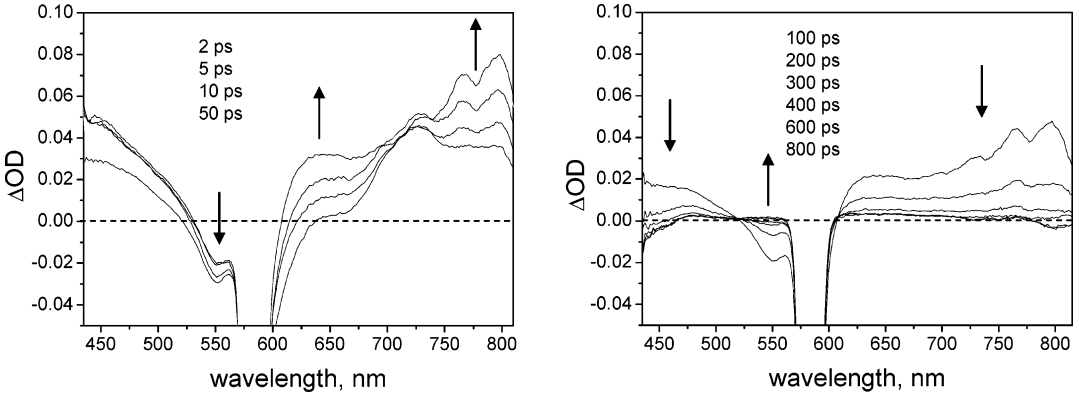

Figure 4. Ultrafast spectroscopy of $(ZnP)_2PBI$ in dichloromethane (excitation at 590 nm): (a) $t \leq 50$ ps, (b) $t \geq 50$ ps.

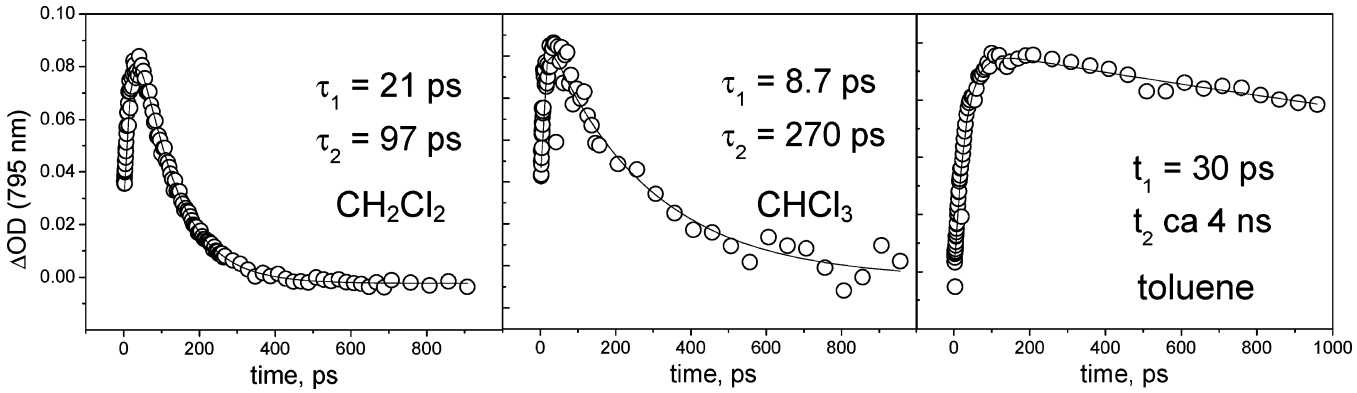

Figure 5. Solvent dependence of the picosecond kinetics of $(ZnP)_2PBI$ (excitation at 590 nm).

ps as the lower detection limit. From the energy-level diagram of Figure 2, the process responsible for the effective quenching of the perylene bisimide excited singlet state is very likely electron transfer leading to the charge-separated product $*PBI(S_1) \rightarrow PBI^- - ZnP^+$.

Experimental proof and kinetic characterization of the electron-transfer quenching can be obtained by femtosecond spectroscopy with 590 nm excitation (corresponding to selective excitation of the perylene bisimide unit). The transient spectral changes obtained in dichloromethane upon excitation at 590 nm of $(ZnP)_2PBI$ are shown in Figure 4. The behavior is clearly biphasic with different spectral changes taking place in the $t \leq 50$ ps (Figure 4a) and $t \geq 50$ ps (Figure 4b) time ranges. The initial spectrum of Figure 4a, taken immediately after the excitation pulse (without correction for spectral chirp), is the typical spectrum of the perylene bisimide singlet state,[19] showing, besides positive absorption in the long and short wavelength region, ground-state bleaching in the 500−600 nm range and stimulated emission in the 600−700 nm range. In the spectral changes of Figure 4a, clear features are (1) the disappearance of the perylene bisimide excited state as shown by the decrease in stimulated emission in the 600−700 range and (2) formation of the reduced form of the perylene bismide chromophore as shown by the rise of the typical absorption at 800 nm.[19] This provides direct evidence for the charge separation process $*PBI(S_1) \rightarrow PBI^- - ZnP^+$. In the longer time scale, Figure 4b, the charge-separated state converts cleanly to the ground state as shown by the return to the initial baseline with good isosbestic points at zero differential absorbance. Kinetic analysis of the spectral changes of Figure 4 at 790 nm (Figure 5a) yields the time constants for charge separation, 21 ps, and charge recombination, 97 ps.

The effect of solvent polarity on these electron-transfer processes has been checked by comparing the results in dichloromethane ($\epsilon = 8.93$) with those of analogous femtosecond experiments (excitation at 590 nm) carried out in chloroform ($\epsilon = 4.81$) and toluene ($\epsilon = 2.38$). While the spectral changes are qualitatively the same in the three solvents, the kinetics is strongly solvent dependent (Figure 5). This is particularly true for the charge recombination process, which slows down monotonically with decreasing solvent polarity. As a consequence, the lifetime of the charge-separated state extends into the nanosecond time scale in toluene. The charge separation process, on the other hand, remains in the time scale of few tens of picoseconds in all solvents with minor lifetime changes that do not correlate monotonously with solvent polarity (experimental order: chloroform < dichloromethane < toluene). The solvent effects can be qualitatively explained in terms of standard electron transfer theory (vide infra).

The fate of long-lived charge-separated state observed by femtosecond spectroscopy in toluene was further investigated using nanosecond laser flash photolysis. The spectral changes in the nanosecond time domain consist of three temporally distinct sets (Figure 6). The initial spectrum, recorded right at the maximum of the excitation pulse (Figure 6a), superimposable to the final spectrum of the ultrafast experiment, corresponds to the $PBI^- - ZnP^+$ charge-separated state. This transient decays in the same time scale as excitation pulse, with apparent lifetime 8 ns, to a new spectrum lacking completely the red absorption of PBI^- while still retaining some bleaching of the ground-state PBI absorption (Figure 6a). We assign this spectrum to a mixture of ZnP and PBI triplet states, given the similarity with the known spectrum of $*PBI(T_1)$,[19] with the presence of an additional absorption at 470 nm typical of $*ZnP(T_1)$.[22] The extra absorption at 470 nm disappears in the time scale 22−65 ns (lifetime, 30 ns) leaving the pure $*PBI(T_1)$ spectrum (Figure 6b, d). The PBI triplet then decays back to the ground state (isosbestic points at $\Delta OD = 0$) with a lifetime of 360 ns in

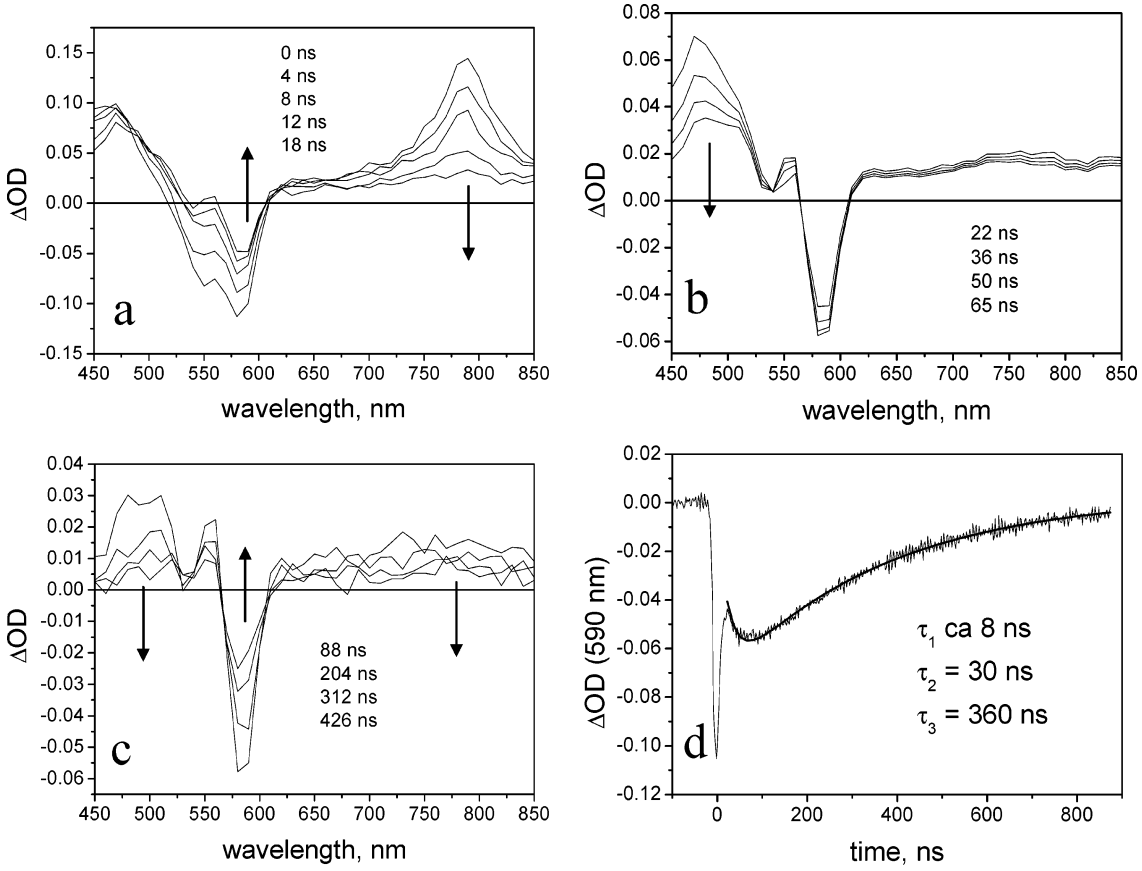

Figure 6. Nanosecond flash photolysis of $(ZnP)_2PBI$ in toluene (excitation at 532 nm): (a) $t = 0-20$ ns, (b) $t = 22-65$ ns, (c) $t = 88-426$ ns, (d) kinetic trace at 590 nm.

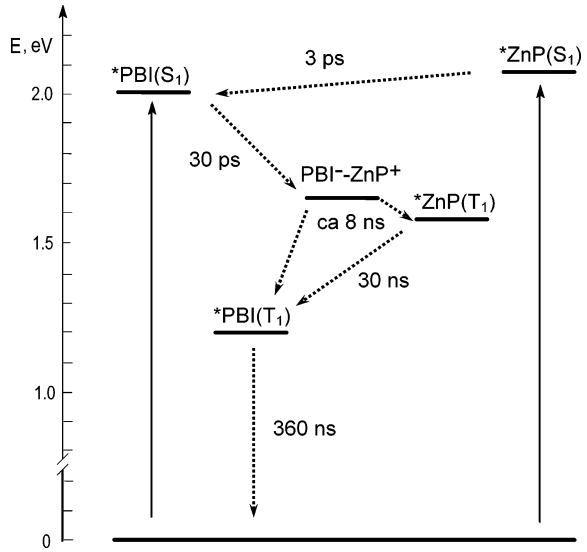

Figure 7. Approximate energy-level diagram and photophysical processes of $(ZnP)_2PBI$ in toluene.

aerated solution (Figure 6c, d). The photophysical mechanism in toluene is schematized in the energy-level diagram of Figure 7 (where a very approximate value for the energy of the charge-separated state is obtained with electrostatic corrections[26] to the experimental redox potentials measured in dichloromethane). The comparison with the analogous scheme for dichloromethane (Figure 2) shows the drastic change in mechanism caused by the change in energy of the charge-separated state. The charge-separated state is initially formed by photoinduced electron transfer in a singlet spin state. In dichloromethane, the allowed charge recombination to the ground state takes place rapidly and with 100% efficiency. In toluene, on the other hand, such a process is expected to be much slower on the basis of electron-transfer theory (vide infra). Thus, the charge-separated state can undergo spin inversion[15b] and yields triplet states upon charge recombination.

Photophysics of $(H_2P)_2PBI$. The absorption spectrum in dichloromethane of $(H_2P)_2PBI$ is compared in Figure 8 with those of the DPyPBI and H_2TPP fragment models. Again, aside from small differences in the band intensities, the spectrum of the adduct is a good superposition of those of the molecular components indicating weak intercomponent interaction and permitting reasonable estimates of the amount of light absorbed by the two types of chromophores at the various wavelengths. For instance, efficient (ca. 80%) excitation of the perylene chromophore is achieved at 585 nm, while efficient (ca. 75%) absorption by the porphyrin chromophore can be obtained at 517 nm. Again, the spectral features remain almost unchanged by changing the solvent from dichloromethane to toluene except for the small blue shift (from 586 to 578 nm) of the perylene bisimide absorption band.

The energy-level diagram for $(H_2P)_2PBI$ is shown in Figure 9 with singlet energies from the fluorescence of DPyPBI and H_2TPP and triplet energies from literature data[19,21] on the same model systems. The energy of the charge-separated state where the free-base porphyrin is oxidized and the perylene bisimide unit is reduced (1.57 eV) is calculated from the known redox potentials of DPyPBI (−0.69 vs SCE in CH_2Cl_2 vide supra) and H_2TPP (0.99 V vs SCE in CH_2Cl_2)[8] with appropriate correction for the electrostatic work term estimated according to standard procedures.[26] With respect to the energy-level diagram for $(ZnP)_2PBI$, the main difference lies in reversal of the energy gap between porphyrin and perylene bisimide singlet

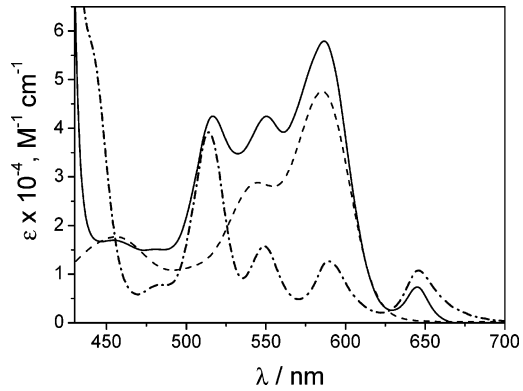

Figure 8. Absorption spectra of $(H_2P)_2PBI$ (continuous line), DPyPBI (dashed line), and H_2TPP (dash−dot line, molar absorptivity values × 2) in dichloromethane.

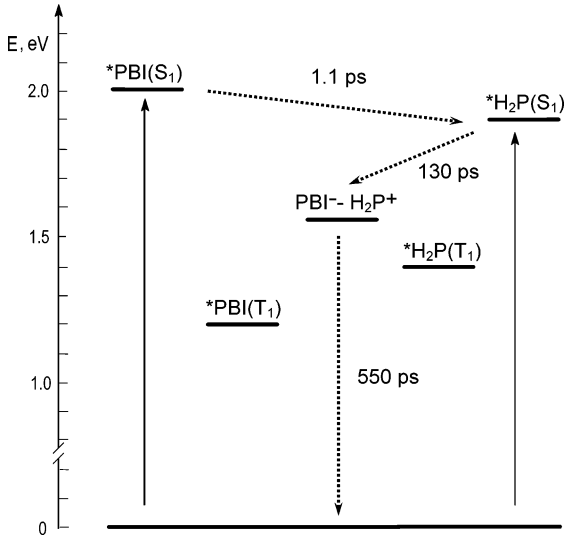

Figure 9. Energy-level diagram for $(H_2P)_2PBI$ in dichloromethane. Observed intramolecular photophysical processes (see below) are indicated by dotted arrows.

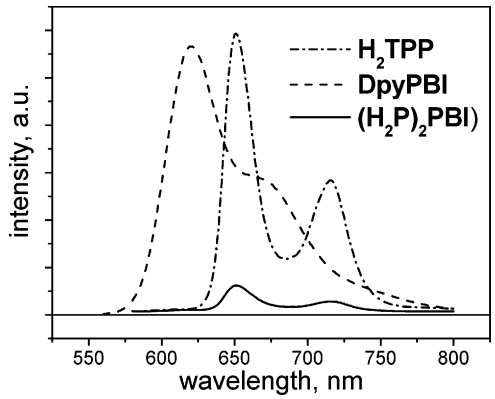

Figure 10. Emission spectra of $(H_2P)_2PBI$ (continuous line), DPyPBI (dashed line), and H_2TPP (dash−dot line) in dichloromethane.

levels. Thus, singlet energy transfer is energetically allowed from perylene bisimide to the free-base porphyrin, while electron-transfer quenching is substantially exergonic for both excited chromophores.

The emission spectra of $(H_2P)_2PBI$, DPyPBI, and H_2TPP in dichloromethane are compared in Figure 10. It is clearly seen that the weak (see below) emission of $(H_2P)_2PBI$ is fluorescence from the porphyrin chromophore. The excitation spectrum of this emission (see Figure S3 of Supporting Material) is superimposable to the absorption spectrum of $(H_2P)_2PBI$ in the whole spectral region of Figure 8. This indicates that singlet energy transfer from the perylene bisimide unit to the porphyrin chromophores, $^*PBI(S_1) \rightarrow {}^*H_2P(S_1)$ in Figure 9, is efficient. Indeed, the process is expected[28,30] and is experimentally found (see below) to be ultrafast (ca. 1 ps). It must be stressed that the porphyrin fluorescence in $(H_2P)_2PBI$ is much weaker than that of free H_2TPP with a quenching ratio greater[31] than 20 being estimated from optically matched solutions. From the energy-level diagram of Figure 9, the process responsible for the effective quenching of the porphyrin excited singlet state is very likely electron transfer leading to the charge-separated product $^*H_2P\ (S_1) \rightarrow PBI^- - ZnP^+$.

The transient spectral changes obtained upon excitation at 585 nm of $(H_2P)_2PBI$ in dichloromethane solution are shown in Figure 11. The spectral changes are clearly triphasic with different spectral changes taking place in the 0−10 (Figure 11a), 10−400 (Figure 11b), and 400−1000 (Figure 11c) time ranges. The initial spectrum of Figure 11a, taken immediately after the excitation pulse, is the typical spectrum of the perylene bisimide singlet state,[19] showing, besides positive absorption in the long and short wavelength region, ground-state bleaching in the 500−600 nm range and stimulated emission in the 600−700 nm range. In the spectral changes of Figure 11a, the disappearance of the perylene bisimide excited state is accompanied by the formation of the typical spectrum of the singlet excited state of the free-base porphyrin,[2o] characterized by bleaching of the four ground-state Q-bands at 520, 550, 590 (hidden within laser pump), and 650 nm (see absorption spectrum of H_2TPP in Figure 8) and by an apparent bleaching at 720 nm corresponding to stimulated emission (see emission spectrum of H_2TPP in Figure 10), superimposed on a relatively positive absorption. This provides direct evidence for the singlet energy transfer process $^*PBI(S_1) \rightarrow {}^*H_2P(S_1)$. Kinetic analysis of the spectral changes of Figure 11a at 760 nm (Figure 11d) yields a time constant for singlet energy transfer of 1.1 ps. The spectral changes in the 10−200 ps time scale (Figure 11b) are indicative of a charge separation process leading to $PBI^- - H_2P^+$. The bleaching of the ground-state Q-bands persists (these features are common to the excited state and to the radical cation of the porphyrin) while stimulated emission at 720 nm disappears and the typical absorption of the perylene bisimide radical anion[19] grows in at 700−800 nm. The kinetic analysis of this process (Figure 11e) gives a time constant of 130 ps for the charge separation process. On a longer time scale (Figure 11c), the transient spectrum decays uniformly at all wavelengths indicating disappearance of the charge-separated state by charge recombination to the ground state. Kinetic analysis (Figure 11e) gives a time constant for charge recombination of 550 ps. The lack of observation of PBI triplet products indicates that charge recombination, though slower than in the $(ZnP)_2PBI$ case, is still too fast for spin inversion to take place in the charge-separated state. The mechanism and time constants are summarized in Figure 9.

The spectral changes obtained in the ultrafast spectroscopy of $(H_2P)_2PBI$ in toluene are very similar in the 1−10 ps range to those reported in Figure 11a for dichloromethane indicating again the occurrence of a fast singlet energy transfer process $^*PBI(S_1) \rightarrow {}^*H_2P(S_1)$ with time constant of ca. 1 ps. In the 10−1000 ps time range, however, no further spectral changes are observed indicating that, contrary to what happens in dichloromethane, the singlet state of the porphyrin unit is not appreciably quenched in toluene. This is confirmed by fluorescence that has practically the same lifetime (9.4 ns) as in the H_2TPP model under comparable conditions. The lack of

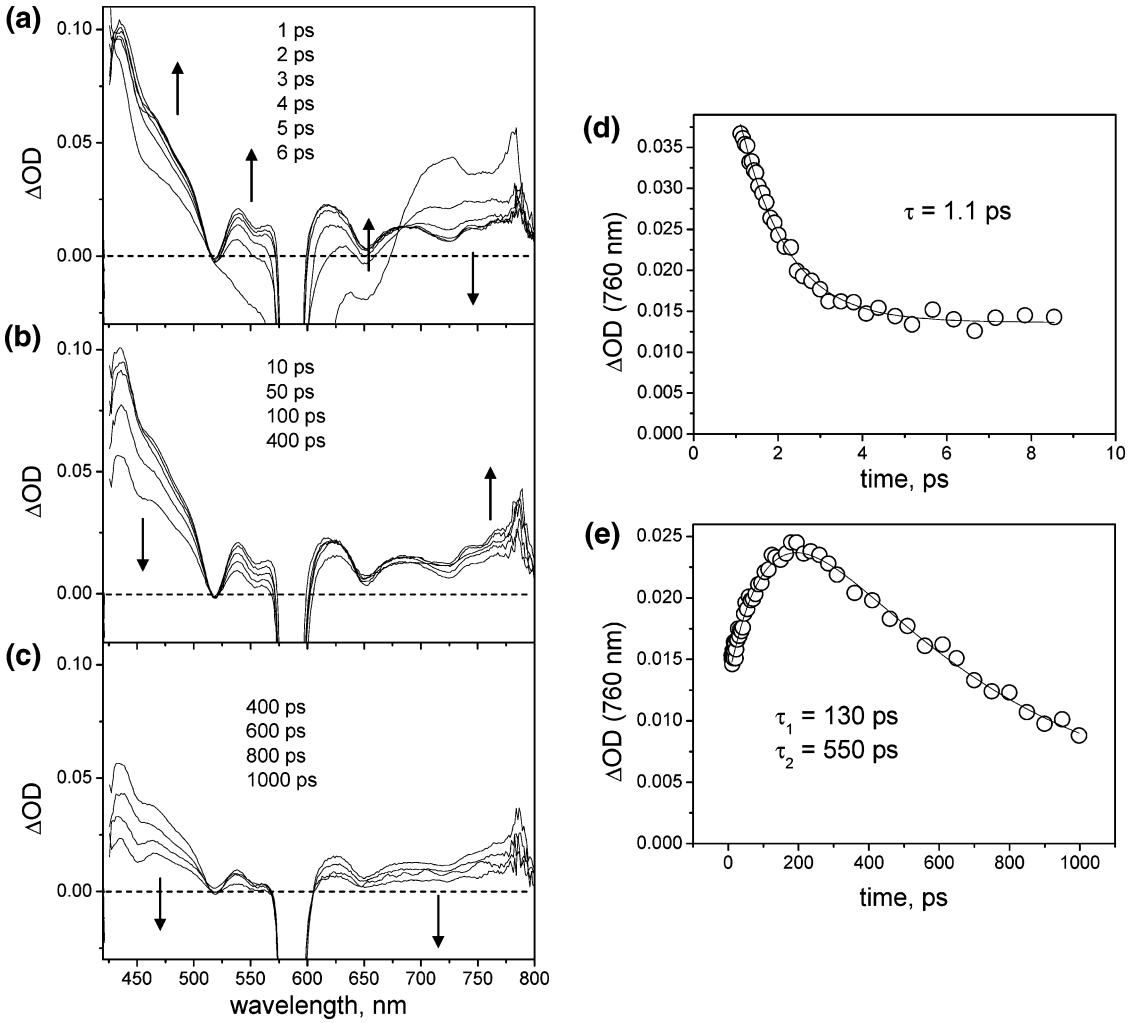

Figure 11. Ultrafast spectroscopy of $(H_2P)_2PBI$ in dichloromethane (excitation at 590 nm). Time-resolved spectra: (a) $t < 10$ ps, (b) $10 \leq t \leq 400$ ps, (c) $t \geq 400$ ps. Kinetics: (d) $t < 10$ ps, (e) $t > 10$ ps.

quenching is in line with the expected increase in energy of the charge-separated state in the less polar solvent. The fate of the $^*H_2P(S_1)$ can be monitored by nanosecond flash photolysis (Figure 12). The initial spectrum of Figure 12a, with bleaching of the porphyrin Q-bands (in particular of the intense band at 520 nm, see Figure 8) and prominent fluorescence at 650 and 770 nm (see Figure 10), is typical of the $^*H_2P(S_1)$ state. In the decay of this transient, taking place largely with the laser pulse (i.e., time constant of ca. 10 ns), the porphyrin fluorescence bands disappear while the porphyrin ground-state bleach persists (Figure 12a). This is indicative of the conversion by intersystem crossing of $^*H_2P(S_1)$ to $^*H_2P(T_1)$. Then, in a longer time scale (Figure 12b), a new transient develops, lacking the porphyrin ground-state bleaching at 520 nm but with a new bleaching at 580 nm, corresponding to perylene bisimide ground-state absorption (see Figure 8). This identifies the process as a triplet−triplet energy transfer from the porphyrin to the perylene bisimide unit. Then, in an even longer time scale (Figure 11c), the perylene bisimide triplet decays to the ground state as indicated by the isosbestic points at $\Delta OD = 0$.

The time constants for the last two processes can be obtained from kinetic fits (Figure 12d). The mechanism for $(H_2P)_2PBI$ in toluene is sketched on the energy-level diagram of Figure 13 (where an approximate value for the energy of the charge-separated state is estimated with electrostatic corrections[26] to the experimental redox potentials measured in dichloromethane).

Electron-Transfer Kinetics. Several electron-transfer processes have been observed in the photophysical study of $(ZnP)_2PBI$ and $(H_2P)_2PBI$ (Figures 2, 7, 9, 13). In principle, the kinetics of these processes can be rationalized in terms of standard electron transfer theory[32] by where the electron-transfer probability is given by a "golden rule" expression of the type

$$k = \frac{2\pi}{\hbar} H_{DA}{}^2 \mathrm{FCWD} \tag{1}$$

where H_{DA} is the electronic coupling between donor and acceptor and FCWD is a thermally averaged nuclear Franck−Condon factor. In a simple approximation in which the solvent modes are thermally excited and treated classically, and a single quantum internal mode of frequency, ν_i is considered, the FCWD term is given by[32a,d]

$$\mathrm{FCWD} = \left(\frac{1}{4\pi\lambda_o k_B T}\right)^{1/2} \sum_m S^m \frac{e^{-S}}{m!} \exp\left[-\frac{(\Delta G^0 + \lambda_o + mh\nu_i)^2}{4\lambda_o k_B T}\right] \tag{2}$$

$$S = \frac{\lambda_i}{h\nu_i} \tag{3}$$

In eq 2, the summation extends over m, the number of quanta of the inner vibrational mode in the product state, ΔG^0 is the

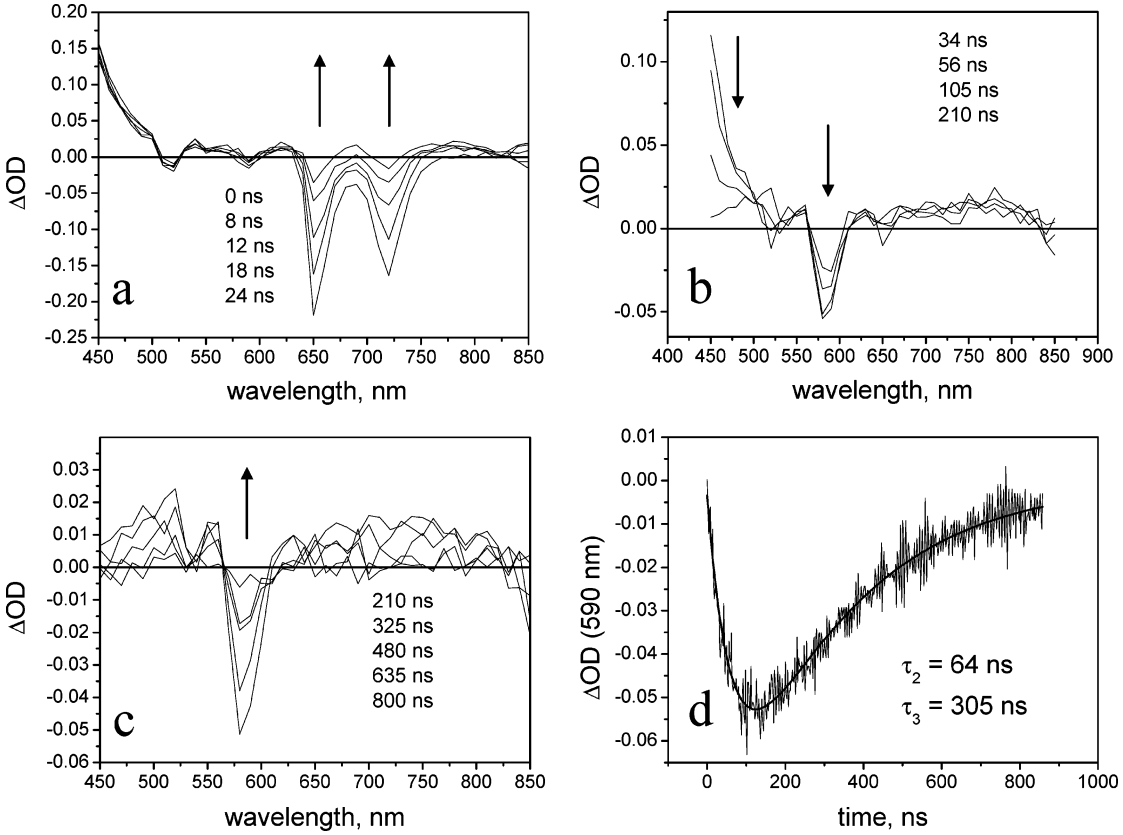

Figure 12. Nanosecond flash photolysis of $(H_2P)_2PBI$ in toluene (excitation at 532 nm): (a) $t = 0-24$ ns, (b) $t = 34-210$ ns, (c) $t = 210-800$ ns, (d) kinetic trace at 590 nm.

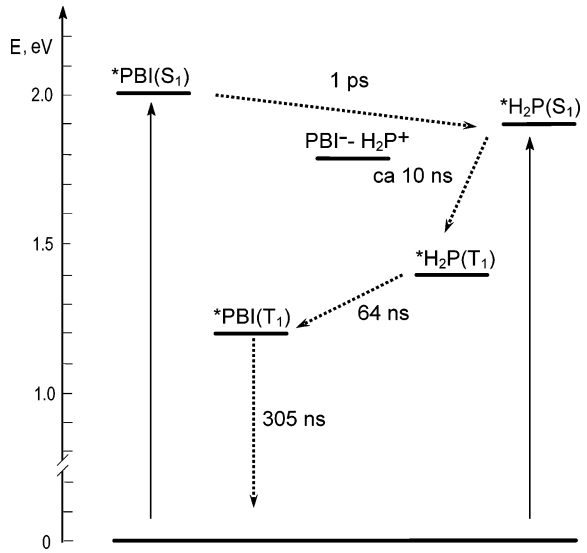

Figure 13. Approximate energy-level diagram and photophysical processes of $(H_2P)_2PBI$ in toluene.

thermodynamic driving force of the process, S is a dimensionless inner-spere reorganizational parameter (eq 3), and λ_o is the outer-sphere (solvent) reorganizational energy given in its simplest form by

$$\lambda_o = e^2\left(\frac{1}{2r_A} + \frac{1}{2r_B} - \frac{1}{r_{AB}}\right)\left(\frac{1}{D_{op}} - \frac{1}{D_s}\right) \qquad (4)$$

where e is the electron charge, D_{op} and D_s are the optical and static dielectric constants of the solvent, r_A and r_B are the radii of the two molecular components, and r_{AB} is the intercomponent distance. For a homogeneous series of processes (where H_{AB}, ν_i, S, and λ_o can be considered appreciably constant), eqs 1−3 provide a correlation between the rate constants and the driving force of electron transfer.

The four processes observed in dichloromethane (eqs 5−8), for which driving force values are known with reasonable accuracy, can be used for checking such a correlation.

$$ZnP-{}^*PBI \rightarrow ZnP^+-PBI^- \quad \Delta G = -0.54 \text{ eV}, \quad k = 4.76 \times 10^{10}\ s^{-1} \qquad (5)$$

$$ZnP^+-PBI^- \rightarrow ZnP-PBI \quad \Delta G = -1.46 \text{ eV}, \quad k = 1.03 \times 10^{10}\ s^{-1} \qquad (6)$$

$${}^*H_2P-PBI \rightarrow H_2P^+-PBI^- \quad \Delta G = -0.33 \text{ eV}, \quad k = 7.69 \times 10^{9}\ s^{-1} \qquad (7)$$

$$H_2P^+-PBI^- \rightarrow H_2P-PBI \quad \Delta G = -1.57 \text{ eV}, \quad k = 1.82 \times 10^{9}\ s^{-1} \qquad (8)$$

A fit of these data according to eqs 1−3 is shown in Figure 14. The set of parameters used is by no means unique particularly as far as the partitioning of the overall reorganization between inner- and outer-sphere contributions is concerned. The fitting is reasonable, however, indicating that the relevant parameters, including the electronic coupling, are appreciably constant in this series of processes regardless of whether charge separation or recombination is considered or whether the porphyrin or perylene bisimide chromophore is excited.

The observed solvent effects on electron-transfer rates, particularly the slowing down of the charge recombination to ground state with decreasing solvent polarity (Figure 5), can be qualitatively explained by the combined effects of (1) changes in driving force and (2) changes in reorganizational energy. As

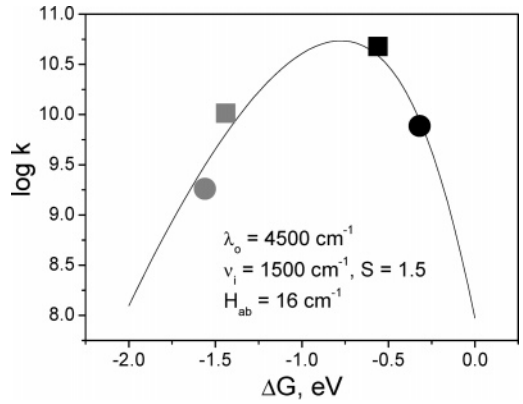

Figure 14. Fit of the rate constants for charge separation (black) and charge recombination (gray) obtained with $(ZnP)_2PBI$ (squares) and $(H_2P)_2PBI$ (dots) in dichloromethane according to eqs 1−3.

the solvent polarity decreases, the energy of the charge-separated state is lifted (Figure 7 vs 2 and Figure 13 vs 9), and the driving force for charge recombination to ground state increases. On the other hand, the reorganizational energy decreases as predicted by eq 4 (e.g., from dichloromethane to toluene, λ_o decreases by a factor of 14). In the Marcus inverted region, where the charge recombination processes belong (Figure 14), both factors act in the same direction predicting a dramatic decrease in rates with decreasing solvent polarity. On the other hand, for the charge separation reactions lying in the normal Marcus region, the two effects tend to compensate, leading to much weaker predicted solvent effects.

Overall, the observed electron-transfer kinetics is satisfactorily accounted for in terms of standard electron transfer theory.

Conclusions

The photophysical behavior of two triads involving two zinc or free-base porphyrins attached to a central perylene bisimide unit has been investigated. Particular attention has been devoted to the effects of solvent polarity, which has been shown to affect not only quantitatively but also qualitatively the photophysical behavior. Because of their symmetric nature, the two triads actually behave as pseudodyads exhibiting a variety of photoinduced energy and electron-transfer intercomponent processes. Using a combination of emission spectroscopy and femtosecond and nanosecond time-resolved absorption techniques, a remarkable number of such processes have been time-resolved and kinetically characterized yielding a very detailed picture of the photophysics of these systems.

The singlet excited state of the lowest energy chromophore (PBI in the case of $(ZnP)_2PBI$, H_2P in the case of $(H_2P)_2PBI$) is always quantitatively populated, besides by direct light absorption, by ultrafast (few ps) singlet energy transfer from the higher energy chromophore.

In dichloromethane, the lowest excited singlet state is efficiently quenched by electron transfer leading to a charge-separated state where the porphyrin is oxidized and the perylene bisimide is reduced. The systems are then brought back to the ground state by charge recombination. The four processes observed for $(ZnP)_2PBI$ and $(H_2P)_2PBI$ in dichloromethane take place in the sub-nanosecond time scale. They nicely obey standard free-energy correlations with charge separation lying in the normal-to-activationless regime and charge recombination in the Marcus inverted region.

In less polar solvents, such as toluene, the energy of the charge-separated states is substantially lifted leading to sharp changes in photophysical mechanism. With $(ZnP)_2PBI$, the electron-transfer quenching is still fast, but charge recombination leads now to triplet state products rather than to the ground state. Spin inversion in the charge-separated state is allowed by the intrinsic slowness (strong Marcus inverted behavior) of the direct process leading to the ground state. Triplet−triplet energy transfer, from the porphyrin to the perylene bisimide, is also involved in the subsequent deactivation of the triplet manifold to the ground state. With $(H_2P)_2PBI$, on the other hand, the driving force for charge separation is apparently too small for electron-transfer quenching. Therefore, the deactivation of the porphyrin excited singlet takes place via intersystem crossing followed by triplet energy transfer to the perylene bisimide and final intersystem crossing to the ground state.

Covalently linked porphyrin−perylene bisimide systems have been previously described. A distinctive aspect of this work lies in the systematic use of energy tuning to affect the photophysical behavior of the systems. To this aim, metalation/demetalation of the porphyrin has been used to change the localization and energy of the lowest excited singlet and to change solvent polarity to shift the energy of the charge-separated state. The photophysical study is quite detailed with a remarkable number of intercomponent processes being spectroscopically detected and kinetically characterized.

Acknowledgment. Financial support from MIUR (Grants FIRB RBNE019H9K and PRIN 2006030320) and Alexander von Humboldt foundation (postdoctoral fellowship for C.-C. You) is gratefully acknowledged.

Supporting Information Available: Fluorescence excitation spectra and additional kinetics (550-nm excitation). This material is available free of charge via the Internet at http://pubs.acs.org.

References and Notes

(1) (a) Wasielewski, M. R. *Chem. Rev.* **1992**, *92*, 435−461. (b) Harriman, A.; Sauvage, J. P. *Chem. Soc. Rev.* **1996**, 41−48. (c) Gust, D.; Moore, T. A.; Moore, A. L. *Acc. Chem. Res.* **1993**, *26*, 198−205. (d) Gust, D.; Moore, T. A.; Moore, A. L. In *Electron Transfer in Chemistry*; Balzani, V., Ed.; Wiley-VCH: Weinheim, Germany, 2001; Vol. III, Part 2, Chapter 2, pp 273−336.

(2) (a) Davila, J.; Harriman, A.; Milgrom, L. R. *Chem. Phys. Lett.* **1987**, *136*, 427−430. (b) Anderson, S.; Anderson, H. L.; Bashall, A.; McPartlin, M.; Sanders, J. K. M. *Angew. Chem., Int. Ed. Engl.* **1995**, *34*, 1096−1200. (c) Prathapan, S.; Johnson, T. E.; Lindsey, J. S. *J. Am. Chem. Soc.* **1993**, *115*, 7519−7520. (d) Hsiao, J.-S.; Krueger, B. P.; Wagner, R. W.; Johnson, T. E.; Delaney, J. K.; Mauzerall, D. C.; Fleming, G. R.; Lindsey, J. S.; Bocian, D. F.; Donohoe, R. J. *J. Am. Chem. Soc.* **1996**, *118*, 11181−11193. (e) Nakano, A.; Osuka, A.; Yamazaki, I.; Yamazaki, T.; Nishimura, Y. *Angew. Chem., Int. Ed.* **1998**, *37*, 3023−3027. (f) Kuciauskas, D.; Liddell, P. A.; Lin, S.; Johnson, T. E.; Weghorn, S. J.; Lindsey, J. S.; Moore, A.; Moore, T. A.; Gust, D. *J. Am. Chem. Soc.* **1999**, *121*, 8604−8614. (g) Anderson, H. L. *Chem. Commun.* **1999**, 2323−2330. (h) Kim, Y. H.; Jeong, D. H.; Kim, D.; Jeoung, S. C.; Cho, H. S.; Kim, S. K.; Aratani, N.; Osuka, A. *J. Am. Chem. Soc.* **2001**, *123*, 76−86. (i) Yang, S. I.; Prathapan, S.; Miller, M. A.; Seth, J.; Bocian, D. F.; Lindsey, J. S.; Holten, D. *J. Phys. Chem. B* **2001**, *105*, 8249−8258. (j) Taniguchi, M.; Ra, D.; Kirmaier, C.; Hindin, E. K.; Schwartz, J. K.; Diers, J. R.; Bocian, D. F.; Lindsey, J. S.; Knox, R. S.; Holten, D. *J. Am. Chem. Soc.* **2003**, *125*, 13461−13470. (k) Takahashi, R.; Kobuke, Y. *J. Am. Chem. Soc.* **2003**, *125*, 2372−2373. (l) Balaban, T. S.; Bhise, A. D.; Fischer, M.; Linke-Schaetzel, M.; Roussel, C.; Vanthuyne, N. *Angew. Chem., Int. Ed.* **2003**, *42*, 2140−2144. (m) Pen, X.; Aratani, T.; Matsumoto, T.; Kawai, T.; Hwang, I.-W.; Ahn, T. K.; Kim, D.; Osuka, A. *J. Am. Chem. Soc.* **2004**, *126*, 4468−4469. (n) Iengo, E.; Zangrando, E.; Bellini, M.; Alessio, E.; Prodi, A.; Chiorboli, C.; Scandola F. *Inorg. Chem.* **2005**, *44*, 9752−9762. (o) Prodi, A.; Chiorboli, C.; Scandola, F.; Iengo, E.; Alessio E. *Chem. Phys. Chem.* **2006**, *7*, 1514−1519. (p) Scandola, F.; Chiorboli, C.; Prodi, A.; Iengo, E.; Alessio E. *Coord. Chem. Rev.* **2006**, *250*, 1471−1496.

(3) (a) Deisenhofer, J.; Epp, O.; Miki, K.; Huber, R.; Michel, H. *J. Mol. Biol.* **1984**, *180*, 385−398. (b) Chang, C.-H.; Tiede, D. M.; Tang, J.; Smith, U.; Norris, J.; Schiffer, M. *FEBS Lett.* **1986**, *205*, 82−86. (c) Allen, J. P.; Feher, G.; Yeates, T. O.; Komiya, H.; Rees, D. C. *Proc. Natl. Acad. Sci. U.S.A.* **1987**, *84*, 5730−5734. (d) Deisenhofer, J.; Michel, H. *Angew.*

Chem., Int. Ed. Engl. **1989**, *28*, 829−847. (e) Huber, R. *Angew. Chem., Int. Ed. Engl.* **1989**, *28*, 848−869.

(4) (a) McDermott, G.; Prince, S. M.; Freer, A. A.; Hawthornthwaite-Lawless, A. M.; Papiz, M. Z.; Cogdell, R. J.; Isaacs, N. W. *Nature* **1995**, *374*, 517−521. (b) Kuehlbrandt, W. *Nature* **1995**, *374*, 497−498. (c) Karrasch, S.; Bullough, P. A.; Ghosh, R. *EMBO J.* **1995**, *14*, 631−638. (d) Kuehlbrandt, W.; Wang, D. N.; Fujiyoshi, Y. *Nature* **1994**, *367*, 614−621. (e) Pullerits, T.; Sundström, V. *Acc. Chem. Res.* **1996**, *29*, 381−389.

(5) (a) Roszak, A. W.; Howard, T. D.; Southall, J.; Gardiner, A. T.; Law, C. J.; Isaacs, N. W.; Cogdell, R. J. *Science* **2003**, *302*, 1969−1972. (b) Bahatyrova, S.; Frese, R. N.; Siebert, C. A.; Olsen, J. D.; van der Werf, K. O.; van Grondelle, R.; Niederman, R. A.; Bullough, P. A.; Otto, C.; Hunter, C. N. *Nature* **2004**, *430*, 1058−1062. (c) Qian, P.; Hunter C. N.; Bullough P. A. *J. Mol. Biol.* **2005**, *349*, 948−960.

(6) Nakamura, Y.; Aratani, N.; Osuka A. *Chem. Soc. Rev.* **2007**, *36*, 831−845.

(7) Kobuke, Y. *Struct. Bonding* **2006**, *121*, 49−104.

(8) You, C-C.; Dobrawa, R.; Saha-Möller, C. R.; Würthner, F. *Top. Curr. Chem.* **2005**, *258*, 39−82.

(9) Drain, C. M.; Goldberg, I.; Sylvain, I.; Falber, A. *Top. Curr. Chem.* **2005**, *245*, 55−88.

(10) Iengo, E.; Scandola, F.; Alessio, E. *Struct. Bonding* **2006**, *121*, 105−143.

(11) Lukas, A. S.; Zhao, Y.; Miller, S. E.; Wasielewski, M. R. *J. Phys. Chem. B* **2002**, *106*, 1299−1306.

(12) Würthner, F. *Chem. Commun.* **2004**, 1564−1579.

(13) (a) Würthner, F.; Thalacker, C.; Sautter, A. *Adv. Mater.* **1999**, *11*, 754−758. (b) Würthner, F.; Thalacker, C.; Sautter, A; Schärtl, W.; Ibach, W.; Hollricher, O. *Chem. Eur. J.* **2000**, *6*, 3871−388. (c) Würthner, F.; Sautter, A.; Schmid, D.; Weber, P. J. A. *Chem. Eur. J.* **2001**, *7*, 894−902. (d) Schenning, A. P. H. J; v. Herrikhuyzen, J.; Jonkheijm, P.; Chen, Z.; Würthner, F.; Meijer, E. W. *J. Am. Chem. Soc.* **2002**, *124*, 10252−10253. (e) You, C.-C.; Würthner, F. *J. Am. Chem. Soc.* **2003**, *32*, 9716−9725. (f) Würthner, F.; Sautter, A. *Org. Biomol. Chem.* **2003**, *1*, 240−243. (g) Sautter, A.; Kaletas, B. K.; D. G.; Schmid, D. G.; Dobrawa, R.; Zimine, M.; Jung, G.; van Stokkum, I. H. M.; De Cola, L.; Williams, R. M.; Würthner, F. *J. Am. Chem. Soc.* **2005**, *127*, 6719−6729. (h) Würthner, F. *Pure Appl. Chem.* **2006**, *78*, 2341−2350.

(14) (a) O'Neil, M. P.; Gaines, G. L., III; Niemczyk, M. P.; Svec, W. A.; Gosztola, D.; Wasielewski, M. R. *Science* **1992**, *257*, 63−65. (b) Hayes T.; Wasielewski, M. R.; Gosztola, D. *J. Am. Chem. Soc.* **2000**, *122*, 5563−5567. (c) Giaimo, J. M.; Gusev, A. V.; Wasielewski, M. R. *J. Am. Chem. Soc.* **2002**, *124*, 8530−8531. (d) Weiss E. A.; Ahrens, M. J.; Sinks, L. E.; Gusev, A. V.; Ratner, M. A.; Wasielewski, M. R. *J. Am. Chem. Soc.* **2004**, *126*, 5577−5584. (e) Ahrens, M. J.; Sinks, L. E.; Rybtchinski, B.; Liu, W.; Jones, B. A.; Giaimo, J. M.; Gusev, A. V.; Goshe, A. J.; Tiede, D. M.; Wasielewski, M. R. *J. Am. Chem. Soc.* **2004**, *126*, 8284−8294. (f) Giaimo, J. M.; Gusev, A. V.; Wasielewski, M. R. *J. Am. Chem. Soc.* **2004**, *126*, 8530−8531. (g) Rybtchinski, B.; Sinks, L. E.; Wasielewski, M. R. *J. Am. Chem. Soc.* **2004**, *126*, 12268−12269. (h) Tauber, M. J.; Giaimo, J. M.; Kelley, R. F.; Rybtchinski, B.; Wasielewski, M. R. *J. Am. Chem. Soc.* **2006**, *128*, 1782−1783.

(15) (a) O'Neil, M. P.; Niemczyk, M. P.; Svec, W. A.; Gosztola, D.; Gaines, G. L., III; Wasielewski, M. R. *Science* **1992**, *257*, 63−65. (b) van der Boom, T.; Hayes, R. T.; Zhao, Y.; Bushard, P. J.; Weiss, E. A.; Wasielewski, M. R. *J. Am. Chem. Soc.* **2002**, *124*, 9582−9590. (c) Kelley, R. F.; Tauber, M. J.; Wasielewski, M. R. *J. Am. Chem. Soc.* **2006**, *128*, 4779−4791. (d) Kelley, R. F.; Shin, W. S.; Rybtchinski, B.; Sinks, L. E.; Wasielewski, M, R. *J. Am. Chem. Soc.* **2007**, *129*, 3173−3181. (e) Ahrens, M. J.; Kelley, R. F.; Dance, Z. E. X.; Wasielewski, M. R. *Phys. Chem. Chem. Phys.* **2007**, *9*, 1469−1478.

(16) (a) Miller, M. A.; Lammi, R. K.; Sreedharan, P.; Holten, D.; Lindsey, J. S. *J. Org. Chem.* **2000**, *65*, 6634−6649. (b) Prathapan, S.; Yang, S. I.; Seth, J.; Miller, M. A.; Bocian, D. F. (c) Holten, D.; Lindsey, J. S. *J. Phys. Chem. B* **2001**, *105*, 8237−8248. (d) Yang, S. I.; Prathapan, S.; Miller, M. A.; Bocian, D. F.; Holten, D.; Lindsey, J. S. *J. Phys. Chem. B* **2001**, *105*, 8249−8258. Yang, S.; Lammi, R. K.; Prathapan, S.; Miller, M. A.; Seth, J.; Diers, J. R.; Bocian, D. F.; Lindsey, J. S.; Holten, D. *J. Mater. Chem.* **2001**, *11*, 2420−2430.

(17) You, C.-C.; Würthner, F. *Org. Lett.* **2004**, *6*, 2401−2404.

(18) Xiao, S.; El-Khouly, M. E.; Li, Y.; Gan, Z.; Liu, H.; Jiang, L.; Araki, Y.; Ito, O.; Zhu, D. *J. Phys. Chem. B* **2005**, *109*, 3658−3667.

(19) Prodi, A.; Chiorboli, C.; Scandola, F.; Iengo, E.; Alessio, E.; Dobrawa, R.; Würthner, F. *J. Am. Chem. Soc.* **2005**, *127*, 1454−1462.

(20) Chiorboli, C.; Rodgers, M. A. J.; Scandola, F. *J. Am. Chem. Soc.* **2003**, *125*, 483−491.

(21) Ford, W. E.; Kamat, P. V. *J. Phys. Chem.* **1987**, *91*, 6373−6380.

(22) Prodi, A.; Indelli, M. T.; Kleverlaan, C. J.; Scandola, F.; Alessio, E.; Gianferrara, T.; Marzilli, L. G. *Chem. Eur. J.* **1999**, *5*, 2668−2679.

(23) In principle, the supramolecular nature of the triads can also be checked by electrochemistry. In practice, the cyclic voltammetry of the triads (dichloromethane, glassy carbon working electrode) is a reasonable superposition of those of the model molecules, but substantial peak broadening and poor reversibility (likely caused by electrode absorption) prevents a precise comparison of potential values.

(24) Converted from original value using $E(\mathrm{Fc/Fc+}) = 0.46$ V versus SCE.[25]

(25) Connelly, N. G.; Geiger, W. E. *Chem. Rev.* **1996**, *96*, 877−910.

(26) (a) Rehm, D.; Weller, A. *Ber. Bunsen−Ges. Phys. Chem.* **1969**, *73*, 834−839. (b) Weller, A. *Z. Phys. Chem.* **1982**, *133*, 93−98. The electrostatic work term in CH_2Cl_2, at an estimated center-to-center distance of 14.8 Å, amounts to 0.11 eV.

(27) Calculated according to Förster[28] with appropriate parameters ($n = 1.424$; $\Phi_D/\tau_D = 1.8 \times 10^7$ s^{-1}; $\kappa^2 = 4$, RDA = 14.8 Å). Calculations performed using PhotochemCAD (Du, H.; Fuh, R. A.; Li, J.; Corkan, A; Lindsey, J. S. *Photochem. Photobiol.* **1998**, *68*, 141−142).

(28) (a) Förster, T. *Ann. Phys.* **1948**, *2*, 55. (b) Förster, T. *Discuss. Faraday Soc.* **1959**, *27*, 7−17.

(29) Femtosecond results obtained with excitation at 550 nm (ca. 60% excitation of the Zn porphyrin chromophore) were practically the same except for small differences in the spectral changes taking place in the first few picoseconds as those reported below for excitation at 590 nm (selective perylene bisimide excitation). The time constant for the conversion of the upper Zn porphyrin chromophores to the lower perylene bisimide by singlet energy transfer, 3.4 ps, can be obtained upon 550 nm excitation by monitoring the decay of the *ZnP(S1) absorption at 440 nm (Figure S2 of supporting material).

(30) With appropriate parameters ($n = 1.424$; $\Phi_D/\tau_D = 1.4 \times 10^8$ s^{-1}; $\kappa^2 = 4$, RDA = 15.8 Å), the calculated time constant is ca. 2 ps. Calculations performed using PhotochemCAD (Du, H.; Fuh, R. A.; Li, J.; Corkan, A; Lindsey, J. S. *Photochem. Photobiol.* **1998**, *68*, 141−142).

(31) A precise quantitative evaluation of the amount of quenching is prevented by the presence of traces of free, unquenched porphyrin as detected by single-photon-counting techniques.

(32) (a) Jortner, J. *J. Chem. Phys.* **1976**, *64*, 4860−4867. (b) Ulstrup, J. *Charge Transfer Processes in Condensed Media*; Springer-Verlag: Berlin, 1979. (c) Marcus, R. A.; Sutin, N. *Biochim. Biophys. Acta* **1985**, *811*, 265−322. (d) Miller, J. R.; Beitz, J. V.; Huddlestone, R. K. *J. Am. Chem. Soc.* **1984**, *106*, 5057−5068. (e) Newton, M. D. *Chem. Rev.* **1991**, *91*, 767−792.